Study of the Catalytic Activity of Calcined Ni/Mg/Al (Mn) Hydrotalcites for N_2O Decomposition*

[a]L. OBALOVÁ, [b]M. VALÁŠKOVÁ, [c]F. KOVANDA, [b]Z. LACNÝ, and [a]K. KOLINOVÁ

[a]*Department of Physical Chemistry and Theory of Technological Processes, Technical University of Ostrava, CZ-708 33 Ostrava*
e-mail: lucie.obalova@vsb.cz

[b]*Institute of Materials Chemistry, Technical University of Ostrava, CZ-708 33 Ostrava*
e-mail: marta.valaskova@vsb.cz

[c]*Department of Solid State Chemistry, Institute of Chemical Technology, CZ-166 28 Prague*
e-mail: Frantisek.Kovanda@vscht.cz

Received 1 April 2003

Mixed oxide-based catalysts prepared by thermal decomposition of Ni—(Mg)—M(III) hydrotalcite-like compounds (M(III) = Al, Mn) were used in catalytic decomposition of nitrous oxide in order to describe the catalytic activity of multicomponent catalysts and to study the effect of Mg^{2+} presence in the catalysts structure. Although the catalytic activity of prepared Ni—Al and Mg—Mn calcined hydrotalcites was high, the simultaneous presence of both transition metal cations Ni^{2+} and Mn^{3+} in the catalyst structure caused a decrease of N_2O conversion and specific surface area. The N_2O conversions decrease with increasing content of Mg in the Ni—Al system and increase in the Ni—Mn system. The rise of Mg content in the catalysts resulted in larger surface area and higher thermal stability of both Ni—(Mg)—Al and Ni—(Mg)—Mn samples. The prepared hydrotalcites as well as calcined products were characterized by the thermal analysis (TG/DTA), powder X-ray diffraction (XRD), and BET surface area measurements.

Nitrous oxide, N_2O, has been considered to be a relatively harmless species for a long time. During the last decade, a growing concern can be noticed since nitrous oxide has been identified as a contributor to the destruction of ozone in the stratosphere and recognized as a relatively strong greenhouse gas. An estimation of nitrous oxide emissions from anthropogenic sources is reported in the range of 1.2×10^6 t year^{-1} [1, 2]. Not all sources are identified yet and the given values may change in the future. The known primary sources of anthropogenic N_2O emissions are, in decreasing order, cultivated soils, chemical industry, stationary and mobile combustion. However, the only emissions that can be reduced in the short term are those associated with combustion (esp. fluidized bed combustion) and chemical processes (*e.g.* adipic and nitric acid production plants, glyoxal and caprolactam productions). A considerable contribution of car engines to the N_2O emissions cannot be neglected and methods for its reducing were also studied [3].

Catalytic decomposition offers an attractive end-of-pipe solution for the abatement of N_2O in waste gases from combustion and chemical industry. The N_2O decomposition was widely studied because this simple reaction was often chosen as a test reaction in developing a correlation between structural and catalytic properties. The state of art in catalytic decomposition of N_2O is well documented in the literature [4—6].

Mixed oxide-based catalysts prepared by thermal treatment of hydrotalcite-like compounds (HTL) have been reported as very active for N_2O decomposition [7—9]. Hydrotalcite-like compounds, a class of layered double hydroxides, consist of positively charged metal hydroxide layers separated from each other by anions and water molecules. Their chemical composition can be represented by the general formula $[M(II)_{1-x}M(III)_x(OH)_2]^{x+}[A^{n-}_{x/n} \cdot yH_2O]^{x-}$, where M(II) and M(III) are divalent and trivalent metal cations, A^{n-} is an n-valent anion, and x has usually values approximately between 0.25 and 0.33 [10]. What makes hydrotalcite a general precur-

*Presented at the 30th International Conference of the Slovak Society of Chemical Engineering, Tatranské Matliare, 26—30 May 2003.

sor is i) its ability to accommodate a large number of bivalent and trivalent cations, ii) the interdispersion of cations on an atomic scale, leading to catalysts with structural homogeneity and without chemical segregation, and iii) the formation of thermostable materials with large surface area upon decomposition.

As reported recently, the combination of two active transition metals Co and Cu present in hydrotalcite structure caused after calcination a spinel formation and increasing catalytic activity in N_2O decomposition [11]. Further, it was published that the presence of Mg in the catalyst prepared by thermal decomposition of cobalt-containing hydrotalcite-like compounds considerably influenced the catalytic behaviour [12]. Therefore, the performance of a new system comprising two transition metals, Ni and Mn, combined with Mg present in hydrotalcite structure was studied in the N_2O catalytic decomposition. Nickel was selected as the calcined Ni—Al hydrotalcite was reported to be active catalyst for N_2O decomposition [8, 13]. The catalytic activity for N_2O decomposition of Mn-containing mixed oxides was also reported [14]. The activity of Mn-systems strongly depends on the oxidation state of manganese; the most active oxidation state of Mn ions dispersed in MgO matrix was Mn^{3+} (compared to Mn^{2+} and Mn^{4+}) [15]. The optimum oxidation state seems to be Mn^{3+} also for the manganese oxides and the activity per unit surface area increases according to the oxidation state of Mn: $MnO < MnO_2 < Mn_3O_4 < Mn_2O_3$ [16].

The aim of this study was the development of active and stable, under industrial conditions, multicomponent catalyst for N_2O decomposition, taking advantage of properties of hydrotalcite structure able to accommodate various bivalent and trivalent cations, *e.g.* Ni—(Mg)—Al and Ni—(Mg)—Mn hydrotalcite-based catalysts.

EXPERIMENTAL

Preparation and Characterization of Catalysts

Samples of Ni—Mg—M (M = Al, Mn) hydrotalcite-like compounds with n(Ni):n(Mg):n(M) ratios of 0:4:2, 4:0:2, 3:1:2, and 2:2:2 (denominated as Mg4M2-HTL, Ni4M2-HTL, Ni3MgM2-HTL, and Ni2Mg2M2-HTL, respectively) were prepared by the standard coprecipitation method [17]. 450 cm^3 of aqueous solution containing appropriate amounts of $Ni(NO_3)_2 \cdot 6H_2O$, $Mg(NO_3)_2 \cdot 6H_2O$, and $Al(NO_3)_3 \cdot 9H_2O$ or $Mn(NO_3)_2 \cdot 4H_2O$ with n(M(II))/n(M(III)) mole ratio of 2 and of total metal ion concentration of 1.0 mol dm^{-3} was added dropwise with vigorous stirring into 200 cm^3 of 0.5 M-Na_2CO_3 solution. The addition took about 1 h. During the synthesis, the temperature was maintained at 25 °C and pH at about 10 by a simultaneous addition of a 3 M-NaOH solution. Then, the resulting suspension was stirred at 25 °C for additional 18 h. The product was filtered off and washed several times with distilled water and dried overnight at 60 °C in air. The dried hydrotalcite-like precursors were formed into extrudates (diameter 3 mm), dried at 130 °C for 4 h and then calcined for 4 h in air at 450 °C. Calcined extrudates were crushed and fraction of particle size 0.100—0.125 mm was used in catalytic measurements. The catalysts prepared from Ni—Mg—Al hydrotalcite-like compounds are signed as Mg4Al2, Ni4Al2, Ni3MgAl2, and Ni2Mg2Al2, respectively and the catalysts prepared from Ni—Mg—Mn hydrotalcite-like compounds are signed as Ni4Mn2, Mg4Mn2, and Ni2Mg2Mn2, respectively.

Thermal analysis (TG/DTA) was carried out using the TG-750 Stanton—Redcroft instrument. Heating rate of 10 K min^{-1}, air flow rate of 10 cm^3 min^{-1}, and 20 mg of corresponding sample were used in these experiments.

The powder X-ray diffraction (XRD) patterns were recorded using XRD powder diffractometer INEL CPS 120 equipped with a curved position-sensitive detector CPS120 (120° 2Θ), reflection mode with a germanium monochromator (to produce Cu$K\alpha_1$ radiation). Silicon powder was used as standard reference material for calibration of CPS detector. Samples were pressed into the flat rotation holder and examined under the same experimental conditions during 2000 s. Voltage applied was 25 kV with 15 mA current. Crystalline phases were identified from the measured XRD patterns using the ICDD-PDF database [18].

The surface area measurements were carried out by nitrogen adsorption at 77 K and evaluated by the one-point BET method. Before the measurement, the samples of prepared catalysts were activated by heating (0.5 h) at 450 °C.

Catalytic Measurements

The N_2O decomposition reaction was performed in fixed-bed stainless steel reactor of 5 mm i.d. in the temperature range 330—450 °C. It was verified that stainless steel did not contribute to the catalyst performance at given reaction conditions. Total flow rate was maintained at 100 cm^3 min^{-1} NTP (273 K, 101 325 Pa). The catalyst bed length was 1 cm and contained 100 mg sample of the catalyst. The space velocity (WHSV) was 60 000 cm^3 g^{-1} h^{-1}. The inlet content of N_2O was 0.1 mole % balanced by He. A temperature-controlled furnace was used for the reactor heating. Prior to each run, the catalysts were pretreated by heating in a He flow of 50 cm^3 min^{-1} at 10 °C min^{-1} up to 450 °C and maintaining this temperature for 1 h. After the pretreatment the feed mixture was passed over the catalysts and the reaction was processed overnight. Then the conversion at 450 °C was measured and the temperature was decreased to the desired level. Generally, 1 h after the change of

Table 1. Chemical Composition of Hydrotalcite-Like Precursors Dried at 60 °C

Sample	w_i/%					Mole ratio n(M(II))/n(M(III))
	Ni	Mn	Mg	Al	Na	
Mg4Al2-HTL	0	0	15.90	9.10	0.027	1.94
Ni4Al2-HTL	35.9	0	0	8.39	0.007	1.96
Ni3MgA12-HTL	27.0	0	3.86	8.43	0.002	1.98
Ni2Mg2Al2-HTL	19.2	0	8.44	9.07	0.002	2.01
Ni4Mn2-HTL	33.0	16.11	0	0	0.007	1.92
Ni2Mg2Mn2-HTL	19.5	16.58	7.12	0	0.140	2.07
Mg4Mn2-HTL	0	22.00	19.42	0	0.378	2.00

Table 2. Properties of Prepared Hydrotalcite-Like Precursors and Catalysts Used for N_2O Decomposition

Sample	Dehydration temperature	Decomposition temperature	S_{BET}*	N_2O conversion
	°C	°C	$m^2\ g^{-1}$	%
Ni4Al2-HTL	120	360	190	79
Ni3MgAl2-HTL	130	390	209	36
Ni2Mg2Al2-HTL	140	390	245	29
Mg4Al2-HTL	215	400	298	1
Ni4Mn2-HTL	160	245	70	8
Ni2Mg2Mn2-HTL	165	270	86	8
Mg4Mn2-HTL	160	295	142	39

*Specific surface area of extrudates calcined at 450 °C. Reaction conditions: 0.1 mole % N_2O in He, m = 0.1 g, flow rate 100 $cm^3\ min^{-1}$.

conditions the N_2O conversion level was constant and considered as the steady state. At least three analyses were averaged for a data point.

The gas chromatograph Hewlett—Packard (model 5890, series II GC) equipped with gas sample loop preceding the split/splitless injector system and electron capture detector was used to analyze the nitrous oxide content in the reactor off-gas. Data were acquired with HP Chemstation. The chromatographic column used was PoraPlot Q (30 m × 0.53 mm × 40 μm). Detection was carried out by an electron capture detector in overheating mode. The 2-point calibration with calibration gases (0.007 mole %, 0.1 mole %) was performed before and after each experimental run.

Application of the experimental tests and the criteria to check the presence of mass and heat transport limitations in the reactor revealed that these restraints were absent [19].

RESULTS AND DISCUSSION

Catalysts Characterization

The results of elemental chemical analysis of the dried hydrotalcite-like precursors are presented in Table 1. The data confirmed the n(M(II))/n(M(III)) mole ratio to be close to the intended value of 2. The prepared precursors contained a small amount of Na cations remaining in the coprecipitated products. Higher Na contents in the Ni2Mg2Mn2-HTL and Mg4Mn2-HTL samples were caused probably due to the insufficient washing.

Two endothermic effects characteristic of hydrotalcite-like compounds can be observed on the DTA curves of all prepared precursors (see Fig. 1). The first one indicated sample dehydration was accompanied by the loss of interlayer water. The second DTA endothermic effect was accounted to the dehydroxylation of hydroxide layers and decomposition of the interlayer carbonate anions. Both dehydration and decomposition temperatures evaluated from DTA measurements are summarized in Table 2.

The highest thermal stability was exhibited by the Mg4Al2-HTL sample, which dehydrated and decomposed at *ca.* 215 °C and 400 °C, respectively. A substitution of Mg^{2+} and Al^{3+} cations by transition metal cations (Ni^{2+} and/or Mn^{3+}) caused a decrease of thermal stability of the precursors. Both dehydration and decomposition temperatures decreased with increasing content of transition metal cations in the hydroxide layers. The substitution of Mg^{2+} cations in Mg—Al hydrotalcite by Ni^{2+} cations decreased especially the dehydration temperature. The interlayer water was probably released gradually in a relatively wide temperature interval because the corresponding DTA peak was rather broad. The second endothermic effect was more distinct.

A gradual decrease of thermal stability with increasing Ni^{2+} content can be observed in Fig. 1. The substitution of Al^{3+} by Mn^{3+} cations decreased con-

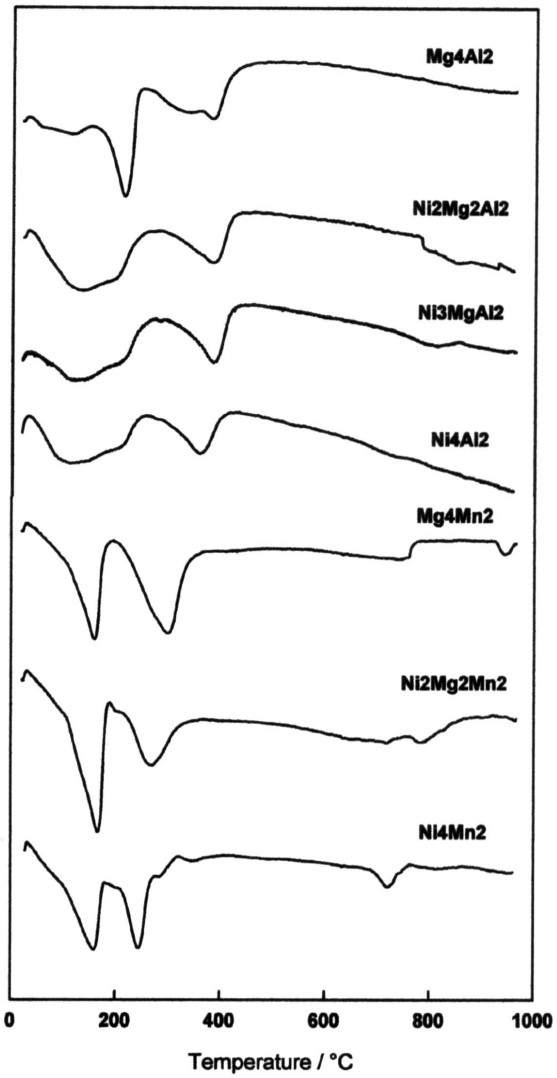

Fig. 1. DTA curves of prepared hydrotalcite-like compounds.

siderably both dehydration and decomposition temperatures of the samples. The lowest thermal stability was exhibited by the Ni4Mn2-HTL sample in which all Mg^{2+} and Al^{3+} cations were substituted by Ni^{2+} and Mn^{3+} cations. A slight endothermic effect at high temperatures (> 700 °C) was detected on DTA curves of Mg4Mn2-HTL, Ni2Mg2Mn2-HTL, and Ni4Mn2-HTL samples, respectively. This effect could be ascribed to a transformation of primary oxides formed after the thermal decomposition of hydrotalcite-like compounds.

The XRD patterns of the prepared Ni—(Mg)—Al and Ni—(Mg)—Mn hydrotalcite samples are demonstrated in Figs. 2*a—c,* and 3*a—c*, respectively. The patterns exhibited the shape characteristic of hydrotalcite-like compounds: the sharp, intense, and symmetric 003, 006, 110, and 113 diffraction lines and less distinct and generally asymmetric 012, 015, and 018 ones, however, owing to the element substitution, the diffraction lines become less sharp. The basal 00*l* reflections correspond to successive orders of the basal spacing and are dependent on the anion size. In the case of two anions in the interlayer region it is possible to observe two different basal reflections corresponding to their combination [20]. The XRD pattern of Mg4Mn2-HTL (Fig. 3*a*) shows out two diffraction lines with *d*-values of 4.566 *Å* and 2.310 *Å* (marked by *), in addition to the typical set of HTL diffractions.

The calcined catalysts were prepared at 450 °C. The powder patterns of Ni—(Mg)—Al samples are in Figs. 2*d—f*. The broad and asymmetric diffraction lines of MgO (periclase) were detected in the pattern of Mg4Al2 catalyst (Fig. 2*d*). The NiO (bunsenite) was identified in the Ni4Al2 catalyst (Fig. 2*e*). The XRD pattern of Ni2Mg2Al2 catalyst (Fig. 2*f*) exhibited also broad and low-intensive diffractions, which could be attributed to the overlapping MgO and/or NiO diffraction lines. The XRD patterns of calcined Ni—(Mg)—Mn samples are in Figs. 3*d—f*. The Mg_6MnO_8 with murdochite structure was detected in Mg4Mn2 catalyst (Fig. 3*d*). The calcination of Ni4Mn2 catalyst was reported in more detail elsewhere [21]. The diffraction lines of the Ni4Mn2 catalyst (Fig. 3*e*) correspond to the Ni_6MnO_8 (murdochite structure). The Ni2Mg2Mn2 catalyst produced in the XRD pattern (Fig. 3*f*) broad diffraction lines corresponding to the $(Ni, Mg)_6MnO_8$ structure and it is in agreement with the (Ni, Mg, Mn(IV)O mixed oxide with disordered murdochite structure detected in this sample earlier [21].

Substituting Mg^{2+} for Ni^{2+} and/or Al^{3+} for Mn^{3+} in Mg4Al2 catalyst results in decreasing catalytic activity in the order: Ni4Al2 > Mg4Mn2 > Ni4Mn2 > Mg4Al2 (Fig. 4). Activity of Mg4Al2 catalyst is very low (1 % N_2O conversion) as it was well documented in literature previously [8, 22]. The Ni4Al2 catalyst was prepared from Mg4Al2 by substitution of Mg^{2+} for Ni^{2+}. The sharp increase of N_2O conversion (79 %) was shown over this catalyst. However, the substitution of Al^{3+} for Mn^{3+} in Mg4Al2 catalyst caused only 39 % N_2O conversion. The further decrease of catalytic performance (8 % N_2O conversion) was observed over Mg4Mn2 catalyst. This sample was prepared from Mg4Al2 by substitution of Mg^{2+} and Al^{3+} for Ni^{2+} and Mn^{3+}, respectively. From these results it followed that catalysts containing both transition metals (Ni and Mn) were relatively inactive although catalysts containing only one of these transition metals were active.

The differences of catalytic activities could be explained by the dissimilar surface area found for Ni4Mn2 catalyst in comparison with Ni4Al2 one. The Ni4Al2 catalyst showed surface area two to three times larger than Ni4Mn2 catalyst (see Table 1). The different catalysts surface area was probably connected with lower thermal stability of the NiMn-HTL precursor in comparison with NiAl-HTL as it was determined from DTA analysis. The dried hydrotalcite-like com-

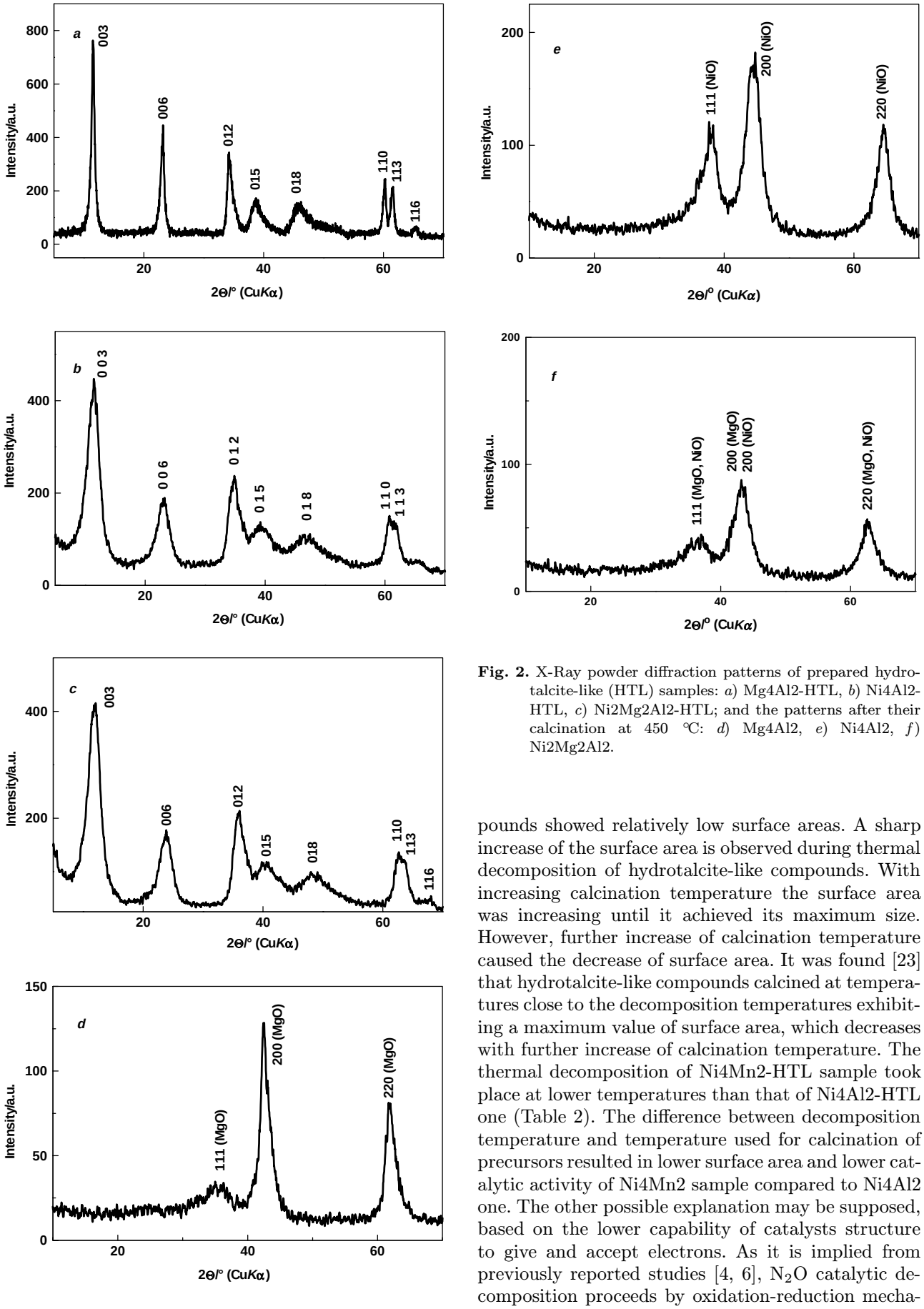

Fig. 2. X-Ray powder diffraction patterns of prepared hydrotalcite-like (HTL) samples: *a*) Mg4Al2-HTL, *b*) Ni4Al2-HTL, *c*) Ni2Mg2Al2-HTL; and the patterns after their calcination at 450 °C: *d*) Mg4Al2, *e*) Ni4Al2, *f*) Ni2Mg2Al2.

pounds showed relatively low surface areas. A sharp increase of the surface area is observed during thermal decomposition of hydrotalcite-like compounds. With increasing calcination temperature the surface area was increasing until it achieved its maximum size. However, further increase of calcination temperature caused the decrease of surface area. It was found [23] that hydrotalcite-like compounds calcined at temperatures close to the decomposition temperatures exhibiting a maximum value of surface area, which decreases with further increase of calcination temperature. The thermal decomposition of Ni4Mn2-HTL sample took place at lower temperatures than that of Ni4Al2-HTL one (Table 2). The difference between decomposition temperature and temperature used for calcination of precursors resulted in lower surface area and lower catalytic activity of Ni4Mn2 sample compared to Ni4Al2 one. The other possible explanation may be supposed, based on the lower capability of catalysts structure to give and accept electrons. As it is implied from previously reported studies [4, 6], N_2O catalytic decomposition proceeds by oxidation-reduction mecha-

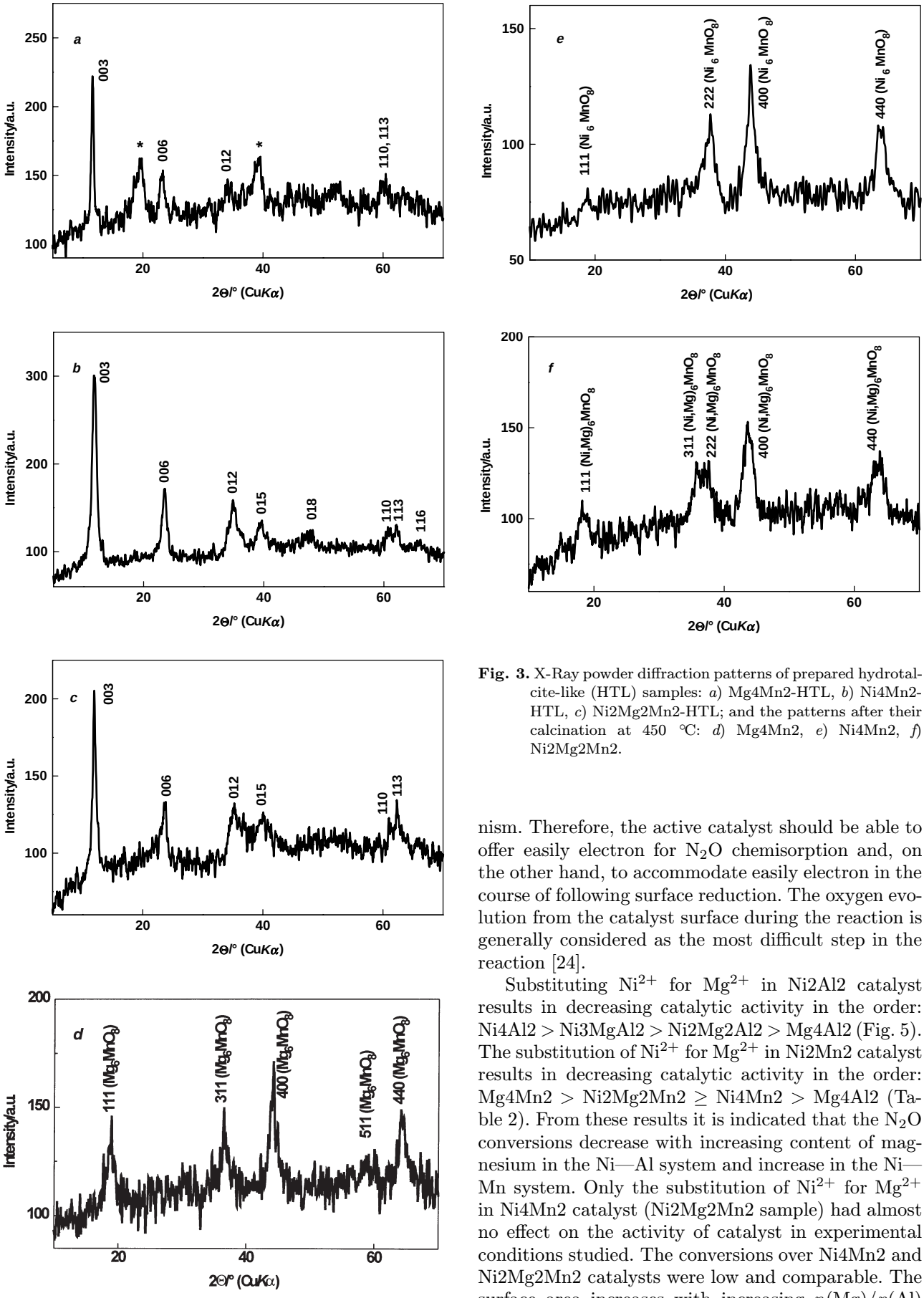

Fig. 3. X-Ray powder diffraction patterns of prepared hydrotalcite-like (HTL) samples: *a*) Mg4Mn2-HTL, *b*) Ni4Mn2-HTL, *c*) Ni2Mg2Mn2-HTL; and the patterns after their calcination at 450 °C: *d*) Mg4Mn2, *e*) Ni4Mn2, *f*) Ni2Mg2Mn2.

nism. Therefore, the active catalyst should be able to offer easily electron for N_2O chemisorption and, on the other hand, to accommodate easily electron in the course of following surface reduction. The oxygen evolution from the catalyst surface during the reaction is generally considered as the most difficult step in the reaction [24].

Substituting Ni^{2+} for Mg^{2+} in Ni2Al2 catalyst results in decreasing catalytic activity in the order: Ni4Al2 > Ni3MgAl2 > Ni2Mg2Al2 > Mg4Al2 (Fig. 5). The substitution of Ni^{2+} for Mg^{2+} in Ni2Mn2 catalyst results in decreasing catalytic activity in the order: Mg4Mn2 > Ni2Mg2Mn2 ≥ Ni4Mn2 > Mg4Al2 (Table 2). From these results it is indicated that the N_2O conversions decrease with increasing content of magnesium in the Ni—Al system and increase in the Ni—Mn system. Only the substitution of Ni^{2+} for Mg^{2+} in Ni4Mn2 catalyst (Ni2Mg2Mn2 sample) had almost no effect on the activity of catalyst in experimental conditions studied. The conversions over Ni4Mn2 and Ni2Mg2Mn2 catalysts were low and comparable. The surface area increases with increasing $n(\mathrm{Mg})/n(\mathrm{Al})$

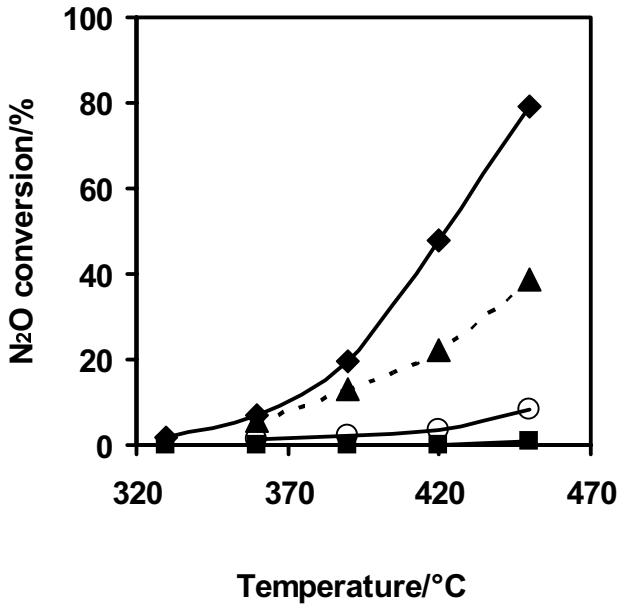

Fig. 4. Conversions of N_2O as a function of temperature. Effect of combination of Ni^{2+} and Mn^{3+}. ♦ Ni4Al2, ▲ Mg4Mn2, ○ Ni4Mn2, ■ Mg4Al2.

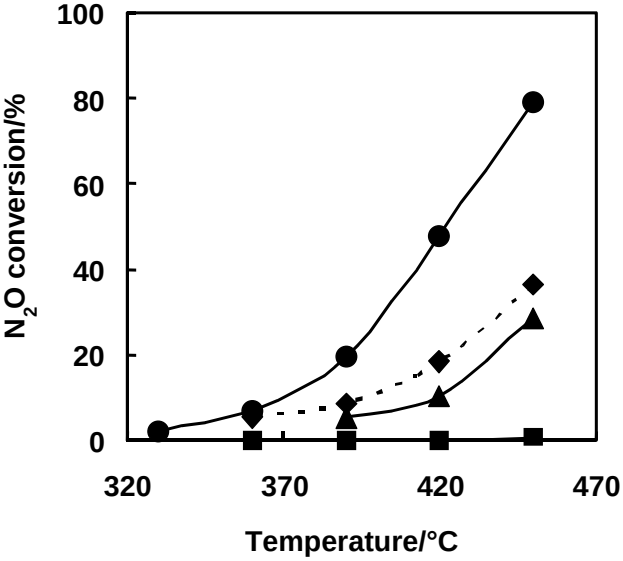

Fig. 5. Conversions of N_2O as a function of temperature. Effect of the Mg^{2+} content in the catalysts structure. ● Ni4Al2, ♦ Ni3MgAl2, ▲ Ni2Mg2Al2, ■ Mg4Al2.

and $n(\mathrm{Mg})/n(\mathrm{Mn})$ ratios in agreement with the results published in [12, 25]. The highest value (298 m^2 g^{-1}) was determined for Mg4Al2 catalyst (Table 2).

The influence of Mg upon catalytic activity observed could be interpreted by the compensation of the following opposite effects: i) The substitution of Ni for Mg in Ni—(Mg)—Al samples led to the decrease of catalytic activity. Ni was a component responsible for the catalytic activity and its replacement by Mg decreased the number of active sites. ii) The presence of Mg increased the thermal stability and surface area, resulting in larger number of exposure surface sites.

The comparison of N_2O conversion for all samples at temperature 450 °C, inlet content 0.1 mole % N_2O in He, and WHSV = 60 000 cm^3 g^{-1} h^{-1} is shown in Table 2. The best result was obtained over Ni4Al2 sample, which exhibits 79 % conversion at 450 °C. Activity of Ni4Al2 is comparable to state-of-the-art catalysts, Fe-zeolites, reported by *Pérez-Ramírez et al.* [24]: 75—88 % conversion at 450 °C, 1500 ppm N_2O in He, GHSV = 60 000 h^{-1}. However, the activity of Ni4Al2 is not stable and it was decreased during our time on stream experiments (460 h). The catalytic activity observed for Mg4Mn2 catalyst (39 % N_2O conversion) was stable during the time on stream measurements. Based on these results we can conclude that the activity of Ni4Al2 catalyst is high and decreasing in time and the activity of Mg4Mn2 is lower but without deactivation observed. Selection of suitable catalyst is almost a compromise between high activity and stability of catalyst. Further experiments will be provided in order to increase catalytic activity of the Mg4Mn2 system and to verify its behaviour in industrial conditions in the presence of O_2, NO_x, and H_2O.

Acknowledgements. This work was supported by the Grant Agency of the Czech Republic (Grant No. 106/02/0523) and by the Czech Ministry of Education, Youth, and Sports (Research Project No. CEZ: MSM 223/10/0002). Authors also thank M. Markvart from the Institute of Inorganic Chemistry of CAS for helpful discussion.

REFERENCES

1. Pérez-Ramírez, J., Kapteijn, F., Schöffel, K., and Moulijn, J. A., *Appl. Catal., B 44*, 117 (2003).
2. *Draft Inventory of U.S. Greenhouse Gas Emissions and Sinks: 1990-1998*. U.S. Environmental Protection Agency, http://www.epa.gov/globalwarming/publications/emissions.
3. Centi, G., Arena, G. E., and Perathoner, S., *J. Catal. 216*, 443 (2003).
4. Kapteijn, F., Rodriguez-Mirasol, J., and Moulijn, J. A., *Appl. Catal., B 9*, 25 (1996).
5. Obalová, L. and Bernauer, B., *Chem. Listy 5*, 255 (2003).
6. Pérez-Ramírez, J., Kapteijn, F., Mul, G., Xu, X., and Moulijn, J. A., *Catal. Today 76*, 55 (2002).
7. Román-Martínez, M. C., Kapteijn, F., Cazorla-Amorós, D., Pérez-Ramírez, P., and Moulijn, J. A., *Appl. Catal., A 225*, 87 (2002).
8. Armor, J. N., Braymer, T. A., Farris, T. S., Li, Y., Petrocelli, F. P., Weist, E. L., Kannan, S., and Swamy, C. S., *Appl. Catal., B 7*, 397 (1996).
9. Kannan, S. and Swamy, C. S., *Catal. Today 53*, 725 (1999).
10. Cavani, F., Trifiro, F., and Vaccari, A., *Catal. Today 11*, 173 (1996).
11. Bo, W., Shugin, W., and Yahui, Z., *Spectrosc. Lett. 30*, 1165 (1997).

12. Pérez-Ramírez, J., Kapteijn, F., and Moulijn, J. A., *Appl. Catal., B 23*, 59 (1999).
13. Obalová, L., Kovanda, F., Chmielová, M., Lacný, Z., and Smetana, B., *Chem. Pap. 56*, 387 (2002).
14. Wang, J., Yasuda, H., Inumaru, K., and Misono, M., *Bull. Chem. Soc. Jpn. 68*, 1226 (1995).
15. Cimino, A. and Indovina, V., *J. Catal. 17*, 54 (1970).
16. Yamashita, T. and Vannice, A., *J. Catal. 161*, 254 (1996).
17. Reichle, W. T., *Solid State Ionics 22*, 135 (1986).
18. PDF 2 database, Internal Centre for Diffraction Data, Newton Square, Pennsylvania, 1996.
19. Ertl, G., Knözinger, H., and Weitkamp, J., *Handbook of Heterogeneous Catalysis*, Vol. *3*. Wiley, Weinheim, 1996.
20. Miyata, S., *Clay Miner. 23*, 369 (1975).
21. Kovanda, F., Grygar, T., and Dorničák, V., *Solid State Sci. 5,* 1019 (2003).
22. Kannan, S., *Appl. Clay Sci. 13*, 347 (1998).
23. Jirátová, K., Čuba, P., Kovanda, F., Hilaire, L., and Pitchon, V., *Catal. Today 76*, 43 (2002).
24. Pérez-Ramírez, J., Kapteijn, F., Mul, G., and Moulijn, J. A., *J. Catal. 208*, 211 (2002).
25. Pérez-Ramírez, J., Mul, G., Xu, X., Kapteijn, F., and Moulijn, J. A., *Stud. Surf. Sci. Catal. 130*, 1445 (2000).